INTERNATIONAL JOURNAL OF HYDROGEN ENERGY 43 (2018) 10980–10990

Available online at www.sciencedirect.com

ScienceDirect

journal homepage: www.elsevier.com/locate/he

A molecular dynamics simulation study of PVT properties for $H_2O/H_2/CO_2$ mixtures in near-critical and supercritical regions of water

Xueming Yang [a,*], *Jiangxin Xu* [a], *Sihan Wu* [a], *Meng Yu* [a], *Bo Hu* [b], *Bingyang Cao* [b,**], *Jiahu Li* [a]

[a] *Department of Power Engineering, North China Electric Power University, Baoding 071003, China*

[b] *Key Laboratory for Thermal Science and Power Engineering of Ministry of Education, Department of Engineering Mechanics, Tsinghua University, Beijing 100084, China*

ARTICLE INFO

Article history:
Received 16 February 2018
Received in revised form
18 April 2018
Accepted 25 April 2018
Available online 21 May 2018

Keywords:
Supercritical water gasification
Coal
PVT properties
Molecular dynamics simulation
Peng-Robinson equation of state
Mixtures

ABSTRACT

Supercritical water gasification technology is an efficient and clean way to use the coal. This technology can convert carbon and hydrogen elements of coal into the mixtures of $H_2O/H_2/CO_2$ that can be used for electricity generation. The acquisition of PVT properties of $H_2O/H_2/CO_2$ mixtures is one of the most critical issues in realizing the design and operation of thermal power generation system using this technology. However, no experimental, theoretical and simulation studies exist regarding the PVT properties of $H_2O/H_2/CO_2$ in the near-critical and supercritical regions of water. In this paper, the molecular dynamics simulations of the PVT properties of H_2O/CO_2 mixtures are carried out and the theoretical calculations are conducted based on the equation of state, and the results are compared with the experimental values. Moreover, the PVT properties for H_2O/H_2 mixtures and $H_2O/H_2/CO_2$ mixtures in the near-critical and supercritical regions of water are predicted using molecular dynamics simulation and compared with the calculation results of the equation of state. The results of this paper are of great significance to the development of supercritical water gasification of coal, and could offer the reference for the application of $H_2O/H_2/CO_2$ mixtures in practical production.

© 2018 Hydrogen Energy Publications LLC. Published by Elsevier Ltd. All rights reserved.

Introduction

Coal has the advantages of large storage capacity and better economy compared with oil and natural gas. Coal gasification has drawn much attraction as efficient and clean coal utilization technologies. The integrated gasification combined cycle (IGCC) is a popular way of coal gasification [1–5]. As traditional coal gasification technology, IGCC converts coal into carbon monoxide and hydrogen at high temperatures with a controlled amount of oxygen and/or steam [6,7]. However, the coal gasifier of IGCC mostly operates in gas environments, so expensive and specialized equipments are necessary for the purification of the raw gas and CO_2 emission reduction [8]. Coal and supercritical water gasification is another promising way of coal gasification [9–16]. Guo et al. [8] proposed a novel thermodynamics cycle power generation system based on coal and supercritical water gasification and

* *Corresponding author.*
** *Corresponding author.*
E-mail addresses: xuemingyang@ncepu.edu.cn (X. Yang), caoby@tsinghua.edu.cn (B. Cao).
https://doi.org/10.1016/j.ijhydene.2018.04.214
0360-3199/© 2018 Hydrogen Energy Publications LLC. Published by Elsevier Ltd. All rights reserved.

multi-staged steam turbine reheated by hydrogen combustion. In their process of coal and supercritical water gasification, the organic matter of coal is completely gasified in supercritical water condition and the elements C, H and O are mainly converted into H_2 and CO_2; N, S and other harmful substance precipitate as inorganic salts. The mixed working medium of supercritical water and clean H_2 and CO_2 flows out of reactor (gasifier) into the steam turbine to generate electricity. The power generation system based on coal and supercritical water gasification has many advantages, such as high coal-electricity efficiency, zero net CO_2 emission and no pollutants, and so on, thus shows good prospects [8,17]. Obtaining the PVT properties of $H_2O/H_2/CO_2$ mixtures is a prerequisite for the design and optimization of a thermodynamic system based on coal and supercritical water gasification.

The PVT properties are the most fundamental thermodynamic properties for compressible fluid. Researchers have conducted a large number of experimental measurements on the PVT properties of common fluids and their mixtures [18–25]. It is very difficult to measure the relationship between the pressure, volume, and temperature of the compressible fluid under extreme circumstances. To investigate the PVT properties of the compressible fluid under high temperature and pressure, two approaches are generally employed: the first adopts theoretical prediction models to expand experimental data [26,27], and the other uses computer simulation [28–31]. The common theoretical predication models of PVT properties can be divided into the cubic equation of state models, thermodynamic perturbation models, perturbed hard chain models and others. Among these models, the Peng–Robinson (PR) equation model is widely used in the calculation of PVT properties due to the relatively high computational accuracy for fluid volumetric properties and thermodynamic properties. Kato et al. [26] reported the binary interaction coefficient of the PR equation of state in calculating the carbon dioxide-*n*-paraffin mixtures. Adrian et al. [27] used PR equation of state to study the phase equilibrium of ternary mixtures of carbon dioxide-water-polar solvent. Belonoshko et al. [28,29] performed molecular dynamics (MD) simulations of PVT properties for pure fluid (water, carbon dioxide, hydrogen, etc.), and their results are in good agreement with those of the theoretical model and experimental results. Although extensive studies have been conducted on the PVT properties for H_2O/CO_2 binary mixtures, to the best of our knowledge, no reports are available assessing PVT properties for $H_2O/H_2/CO_2$ ternary mixtures and H_2O/H_2 binary mixtures in the near-critical and supercritical regions of water. In this paper, the PVT properties of $H_2O/H_2/CO_2$ mixtures and H_2O/H_2 mixtures are predicted via molecular dynamics simulations, and their theoretical prediction models are also discussed.

Methodology

Potentials for molecular dynamics simulation

The potentials and the force fields play an important role in the process of molecular dynamics simulation. Therefore, it is important to select the appropriate potentials and force field models for the MD simulation of prediction on the PVT properties. In this study, the Lennard-Jones potential considering Coulomb's force is adopted, and the expression is as follows:

$$u_{ij} = \sum_{k=1}^{m}\sum_{l=1}^{n}\left\{4\varepsilon_{ij}^{kl}\left[\left(\frac{\sigma_{ij}^{kl}}{r_{ij}^{kl}}\right)^{12} - \left(\frac{\sigma_{ij}^{kl}}{r_{ij}^{kl}}\right)^{6}\right] + \frac{q_i^k q_j^l}{4\pi\varepsilon_0 r_{ij}^{kl}}\right\} \quad (1)$$

where u_{ij} is the interaction potential energy between molecules i and j, ε_{ij}^{kl} and σ_{ij}^{kl} are the interaction parameters of L-J potential which represent the energy parameter and scale parameter, respectively. r_{ij}^{kl} is the distance between atom k and atom l, q_i^k and $q_j^l$are the quantity of electric charge of k and l, respectively. ε_0 is the dielectric constant.

There have been extensive experimental studies on the physicochemical properties of pure water, and the researchers have put forward various force field models of water molecule [32,33]. These models can be divided into two categories: the continuum medium model and the explicit solvent model. The explicit solvent model is widely used in molecular dynamics simulation because of its good certainty and operability. The SPC/E model (one of the explicit solvent model) is widely applied to the simulation of water molecules [32]. Zhang et al. [33] suggest that the SPC/E model can still guarantee its accuracy in the simulation of PVT properties for pure water even when the temperature and pressure reach 1873.15 K and 5.0 Gpa, respectively. In this study, the SPC model [34], SPC/E model [33], and TIP4P-2005 model [35] are adopted and compared in the prediction of the PVT properties for pure water. Researchers have also done many studies on carbon dioxide molecules, and put forward many force field models for describing interaction of CO_2 molecules. The TraPPE [36], EPM2 [37], and MSM3 [38] models are commonly used for the force field model of CO_2 molecules. In this work, we adopt the EMP2 model, which is the modified EPM model improved by Harris et al. [37], to describe the interaction of CO_2 molecules. Unlike the H_2O and CO_2 molecules, the types of the force field model for H_2 is less, and there are two commonly used force field models for H_2, the two-site model [39] and single site model [40]. In fact, the simulation results using these force field models for H_2 are generally in good agreement with the experimental data because of the simple structure. The two-site model is used in this paper. Table 1 shows the force field parameters of the models used in this work.

One of the key to the molecular dynamics simulation for the system with different types of molecules mixed is to select proper potentials for the interactions between these molecules. The Lorentz-Berthelot [41] and Kong [42] rules are the commonly used combining rules which to solve the interaction parameters of the potential. Duan et al. [31] calculated the interaction parameters of H_2O molecule and CO_2 molecule by using these two combining rules. They found that the simulation results of the PVT properties for H_2O/CO_2 mixtures with Lorentz-Berthelot and Kong combining rules are comparable with each other. The Lorentz–Berthelot combining rule is most widely used for its simplicity. Because the EPM2 model use the geometric mean combining rule for interactions between unlike atoms of CO_2 molecules, in this study we adopt the following combining rule which is same as that in Refs.

Table 1 – Force field parameters of the models used in this work.

Molecule	Model	Atom	q(e)	σ(Å)	ε/k_B(K)
H_2O	SPC	O	−0.82	3.166	78.197
		H	0.41	0	0
	SPC/E	O	−0.8476	3.166	78.197
		H	0.4238	0	0
	TIP4P-2005	O	−1.1128	3.1589	93.065
		H	0.5564	0	0
CO_2	EMP2	C	0.6512	2.757	28.129
		O	−0.3256	3.033	80.507
H_2	two-site	H	0	2.72	10

[34,37,43,44]. The geometric mean for ε_{ij}^{kl} and σ_{ij}^{kl} are adopted to calculate the cross-interactions between the unlike Lennard–Jones sites of the CO_2 molecules, while the arithmetic mean of σ_{ij}^{kl} and the geometric mean of $\varepsilon_{ij}^{kl}$are used to calculate the Lennard–Jones interactions in any other case. Its equations are as follows.

$$\varepsilon_{ij}^{kl} = \left(\varepsilon_i^k \varepsilon_j^l\right)^{1/2} \tag{2}$$

$$\begin{cases} \sigma_{ij}^{kl} = \left(\sigma_i^k \sigma_j^l\right)^{1/2} & \text{for } k,l = C_{CO_2}, O_{CO_2} \text{ for the EPM2 model} \\ \sigma_{ij}^{kl} = \frac{1}{2}\left(\sigma_i^k + \sigma_j^l\right) & \text{elsewhere} \end{cases} \tag{3}$$

Molecular simulation details

All the MD simulations are conducted using the LAMMPS software package [45]. The MD simulations are performed for three-dimensional cubic box, and the periodic boundary conditions are applied in all X, Y and Z directions. For all LJ interactions, a cut-off distance of 12 Å was used; A long-range tail correction was applied for van der Waals interactions larger than the cut-off radius. Columbic interactions for two atoms closer than 1.2 nm are calculated directly, while those further are calculated through the particle-particle/particle-mesh (PPPM) algorithm with precision of 10^{-4}. The simulations are carried out under NVT ensemble and using the Nosé-Hoover thermostat to control the temperature of simulation system. The time step is set as 1 fs, and the total simulation time is 80 ps for pure water and 1000 ps for the mixtures. During the simulations, the thermodynamics information is recorded every 500 steps. The number of H_2O molecules is set as 1000 in all simulations, and the molar fraction of H_2 and CO_2 in the system is adjusted by their number in the system. Thereafter, the molar volume is controlled by changing the size of the system box.

Theoretical calculation

In the theoretical calculations of PVT properties for the mixtures, the PR equation of state is adopted, which is modified from the van der Waals equation of state [46]:

$$Z^3 - (1 - B)Z^2 + (A - 3B^2 - 2B)Z - (AB - B^2 - B^3) = 0 \tag{4}$$

$$A = \frac{aP}{R^2T^2} \tag{5}$$

$$B = \frac{bP}{RT} \tag{6}$$

$$Z = \frac{Pv}{RT} \tag{7}$$

where a and b are the parameters of the equation of state, and a is the function of temperature, b is a constant for fixed fluid. When using Eq. (4) to Eq. (7) to calculate the pure fluid, a and b can be solved as follows:

$$a(T) = a(T_c)\alpha(T_r, \omega) = 0.45724\frac{R^2T_c^2}{P_c}\alpha(T_r, \omega) \tag{8}$$

$$b(T) = b(T_c) = 0.0778\frac{RT_c^2}{P_c} \tag{9}$$

$$\alpha(T_r, \omega)^{1/2} = 1 + \xi\left(1 - T_r^{1/2}\right) \tag{10}$$

$$\xi = 0.37464 + 1.54226\omega - 0.26992\omega^2 \tag{11}$$

where T_c is the critical temperature, $T_r = T/T_c$ is the reduced temperature, ω is acentric factor of fluid. The related parameters of H_2O, H_2, and CO_2 used in this paper are from the DIPPR 801 Sample Database [47], and are shown in Table 2.

When the above equations are applied to mixtures, the parameters a and b can be obtained by using the Peng-Robinson mixing rule with the parameters of the each pure components:

$$a = \sum_i \sum_j x_i x_j a_{ij} \tag{12}$$

$$b = \sum_i x_i b_i \tag{13}$$

$$a_{ij} = \left(1 - \delta_{ij}\right) a_i^{1/2} a_j^{1/2} \tag{14}$$

where x_i and $x_j$are the molar fraction of the mixture component i and j, δ_{ij} is the binary interaction coefficient. The selections of binary interaction coefficients have an important effect on the calculation of the properties of mixture via equation of state. There are two methods to determine the binary interaction coefficient, the first method is to use the experimental data to fit the equation of state with high precision, and the second method is to calculate by theoretical correlations with a function of prediction. Meng et al. [48] obtained the binary interaction coefficients of 119 mixtures by fitting the second cross-virial coefficient, and the results showed that the binary interaction coefficient for water and carbon dioxide is 0.167. Nishiumi et al. [49] proposed the interaction coefficient of hydrogen-containing system which

Table 2 – The related parameters of H_2O, H_2 and CO_2 used in this work.

	H_2O	CO_2	H_2
T_c (K)	647.096	304.21	33.19
P_c (Pa)	2.20640E+07	7.38300E+06	1.31300E+06
ω	0.344861	0.223621	−0.21599

is closely related to the temperature of system, and it is adopted in this paper:

$$1-\delta_{ij}=1.224-0.0044T+3.251\times10^{-5}T^2 \quad \text{for} T<461.75K \quad (15)$$

$$1-\delta_{ij}=56.98-0.1655T+1.199\times10^{-4}T^2 \quad \text{for} T\geq461.75K \quad (16)$$

The compression factor Z is a correction factor that must be taken into account when applying the equation of state for the ideal gas to the actual gas, and it indicates the deviation of volume between the actual gas and the ideal gas compressed by the same pressure. The formula of compression factor is as follows:

$$Z=\frac{Pv}{RT} \quad (17)$$

where R is the state constant of ideal gas, and $R = 8.314472\ m^3\ Pa/(mol\cdot K)$.

Results and discussion

In the following sections, the PVT properties for pure water, H_2O/CO_2 binary mixtures and H_2O/H_2 binary mixtures are investigated via MD simulations sequentially, after which the PVT properties for $H_2O/H_2/CO_2$ mixtures in the near-critical and supercritical regions of water are predicted via MD simulations and compared to the PR equation of state. To allow the readers to compare to the data in this work, all the numerical data and uncertainty estimates are provided in Supporting Information.

Pure water

Three force field models—SPC, SPC/E, and TIP4P-2005—are respectively adopted and compared in the simulations of the PVT properties of pure water. The parameters of the force field models are shown in Table 1. Simulation results and errors are shown in Figs. 1 and 2, which are compared with the experimental data [50,51] and the calculation results using IAPWS-IF97 [52–54].

These figures indicate that the maximum error and average error of the SPC/E model are smaller than those of the

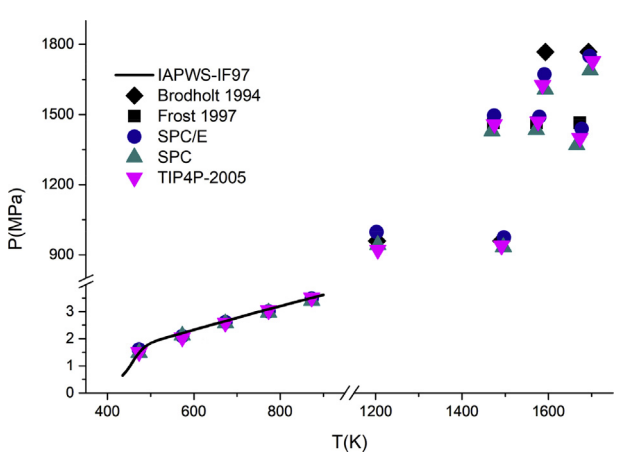

Fig. 1 – Pressure versus temperature for pure water at different molar volumes.

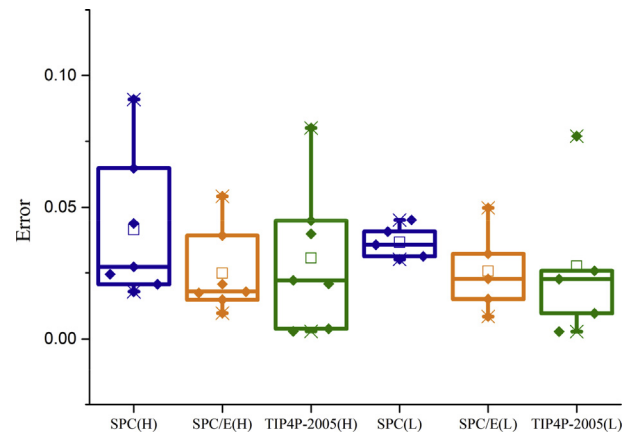

Fig. 2 – Absolute relative deviations of PVT properties for pure water obtained via MD simulations when compared with IAPWS-IF97 values (L) and experimental values (H).

SPC and TIP4P-2005 models, while the maximum uncertainty of the simulation results in the SPC/E model is the smallest. These findings are consistent with conclusions drawn by Zhang [33], wherein SPC/E demonstrates better overall predictions compared to TIP4P, TIP5P, and EP. Therefore, in this study, we choose the SPC/E model for the water molecule model when simulating PVT properties for H_2O/CO_2 binary mixtures, H_2O/H_2 binary mixtures, and the ternary mixtures of $H_2O/H_2/CO_2$ afterwards.

H_2O/CO_2 binary mixtures

The PVT properties of H_2O/CO_2 binary mixtures are simulated and calculated. The results of simulation and the theoretical calculation of H_2O/CO_2 binary mixtures are compared with the experimental values in a temperature range of 350–750 K and pressure range of 0.3–35 MPa. The CO_2 molar fractions (x_{CO_2}) in the mixtures are 20.87%, 39.83%, and 50%, respectively. Fig. 3 shows the simulation results (green up-pointing triangles), P-R equation calculation results (continuous lines), and experimental values [55,56] (blue circles and red squares) of the PVT properties for H_2O/CO_2 binary mixtures at different CO_2 molar fractions. The concentration value corresponding to each experimental value is selected and used in the prediction process using the PR equation of state and MD simulation.

In the case of x_{CO_2} = 50%, the predicted pressure value by both the PR equation of state and MD simulation agree relatively well with the experimental values at different temperatures and concentrations. When x_{CO_2} = 39.83% at a higher temperature and concentrations, the predicted value of the pressure by the PR equation of state and MD simulation are slightly larger than the experimental values, while the average errors of the PR equation of state and MD simulation are 8.93% and 8.56%, respectively. However, when the CO_2 molar fraction is relatively low (x_{CO_2}=20.87%), the absolute average error of the PR equation of state and MD simulation is 15.09% and 0.66%, respectively. Thus, the adopted MD simulation model appears to have much better predictive accuracy than the PR equation of state in near-critical and supercritical regions of water. It should be emphasized the main objective of our

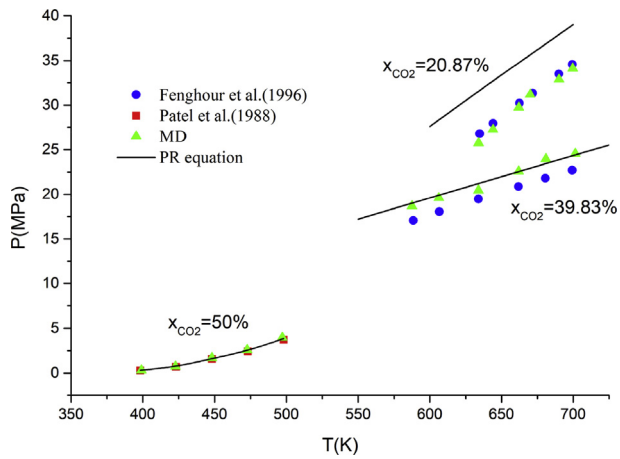

Fig. 3 – Pressure as a function of temperature predicted by simulation and equation of state compared with experimental data for H_2O/CO_2 binary mixtures.

study is to predict the PVT properties for $H_2O/H_2/CO_2$ mixtures in the near-critical and supercritical regions of water. Although some special equation of state [44] can provide more accurate predictions for H_2O/CO_2 binary mixtures, their parameters are evaluated from simulated PVT data or experimental data and thus are not directly applicable to $H_2O/H_2/CO_2$ ternary mixtures.

H_2O/H_2 binary mixtures

To the best of our knowledge, no experimental research has investigated the PVT properties of H_2O/H_2 binary mixtures in the near-critical and supercritical regions of water. Therefore, the results of H_2O/H_2 binary mixtures predicted via molecular dynamics simulations are only compared with the calculated results using the PR equation of state. The simulation results (symbols) and calculation results (lines) of the PVT properties for H_2O/H_2 binary mixtures with molar volumes (υ, L/mol) of 0.213 L/mol, 0.5 L/mol, 1.0 L/mol, and 1.667 L/mol are shown in Fig. 4(a), (b), (c), and (d), respectively.

To clarify the comparison, the absolute relative deviations (ARD) between the MD simulation results and the calculation results using the PR equation of state are calculated as follows:

$$\mathrm{ARD} = \left|\frac{A^{sim} - A^{calc}}{A^{sim}}\right| \times 100\% \tag{18}$$

where $A^{sim}$is the MD simulation value and A^{calc} is the value calculated by the PR equation of state. Fig. 5 (a)–(d) show the ARD corresponding to Fig. 4 (a)–(d), respectively. Both the data and corresponding ARD in Figs. 4 and 5 are provided in Table S3 of the Supporting information. When temperatures increase from 673 K to 923 K at 50 K intervals, the average ARDs for all predictions decrease gradually with the following values: 9.36%, 6.84%, 4.87%, 3.47%, 2.05% and 1.45%; however, it shows a slight increase at 973 K, with a value of 1.77%. Moreover, when molar volumes increase from 0.213 L/mol to 1.667 L/mol, the average ARDs for all predictions decrease rapidly with the following values: 7.96%, 4.32%, 2.62%, and 2.14%. Because the main goal of this work concerns $H_2O/H_2/CO_2$ ternary mixtures, the simulation details for H_2O/H_2 binary mixtures are not provided but will be displayed in the next section in simulations for $H_2O/H_2/CO_2$ ternary mixtures.

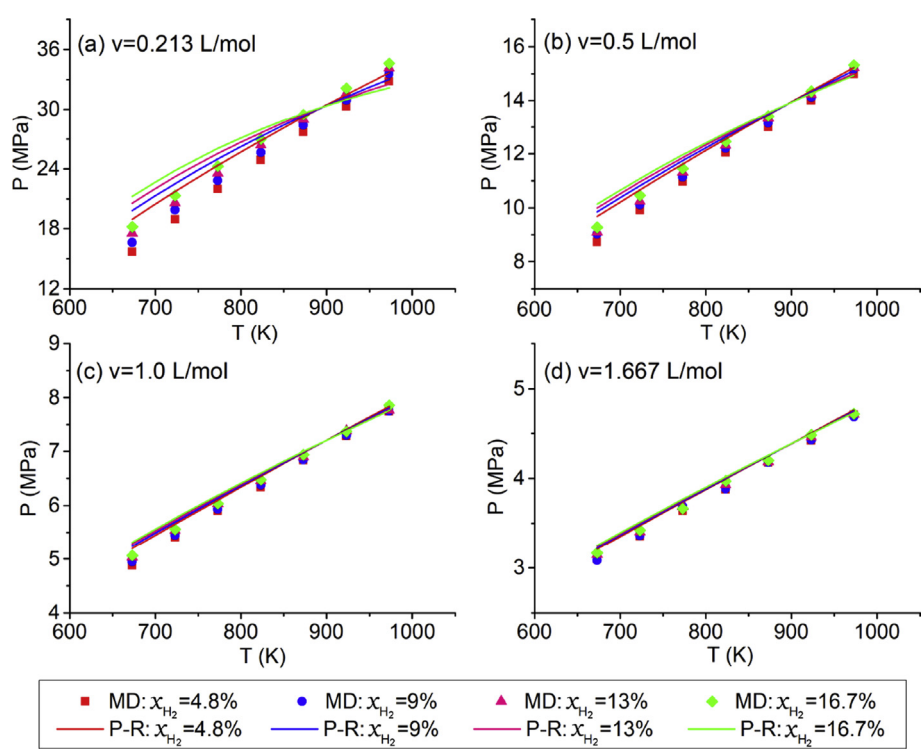

Fig. 4 – Pressure as a function of temperature predicted by the molecular dynamics simulation compared with the theoretical calculation for H_2O/H_2 binary mixtures at different molar volumes.

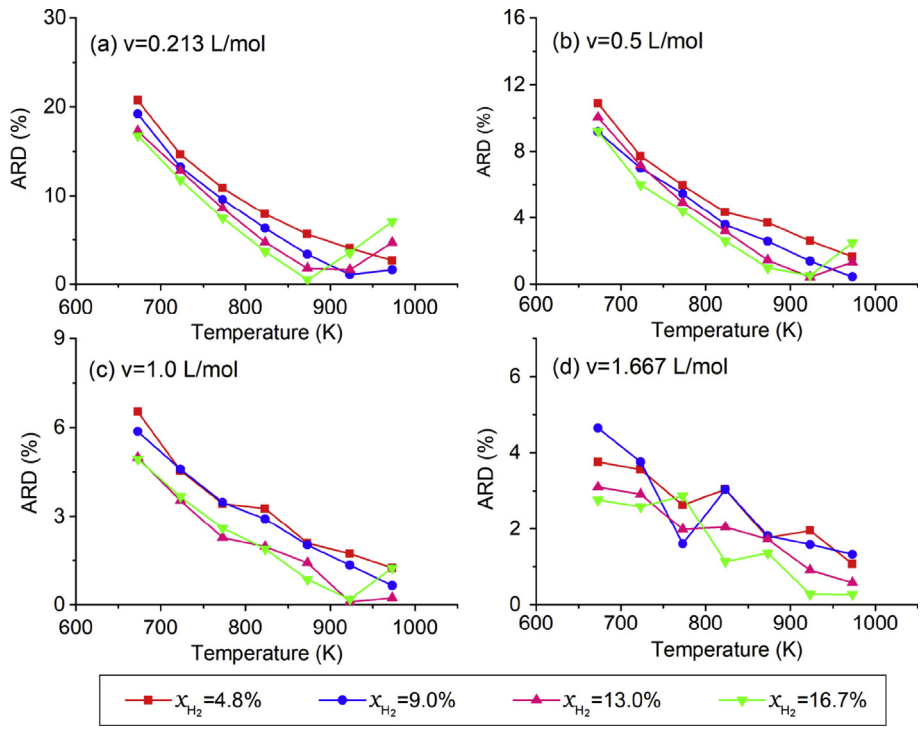

Fig. 5 – ARD as a function of temperature predicted by the molecular dynamics simulation compared with the theoretical calculation for H_2O/H_2 binary mixtures at different molar volumes.

$H_2O/H_2/CO_2$ ternary mixtures

A series of simulations are conducted to predict the PVT properties of $H_2O/H_2/CO_2$ ternary mixtures. To confirm whether the simulation system reached equilibrium, the energies of the mixtures in the simulation process are calculated, and the spatial distribution of the molecules in the mixtures at the end of the simulation is analyzed. For example, Fig. 6(a) shows the energies of the systems at 673 K for the mixtures with 1000 H_2O, 200 H_2, and 200 CO_2 molecules; Fig. 6(b) shows the corresponding spatial distribution of molecules at the end of the simulations.

The energies of the system are in a relatively stable state after reaching a low value in a short period of time, indicating that the mixture system reaches an equilibrium state, and the results obtained by molecular dynamics simulations are not affected by the initial spatial distribution of the molecules. The molecules shown in Fig. 6(b) at 673 K are randomly distributed. To discuss whether system size is playing a role in the simulation, a series of simulations with different system sizes are carried out and results are listed in Table 3. We find that the simulation results are consistent with each other within their uncertainties. The uncertainties decrease with the increase of the system size but this effect seems to be

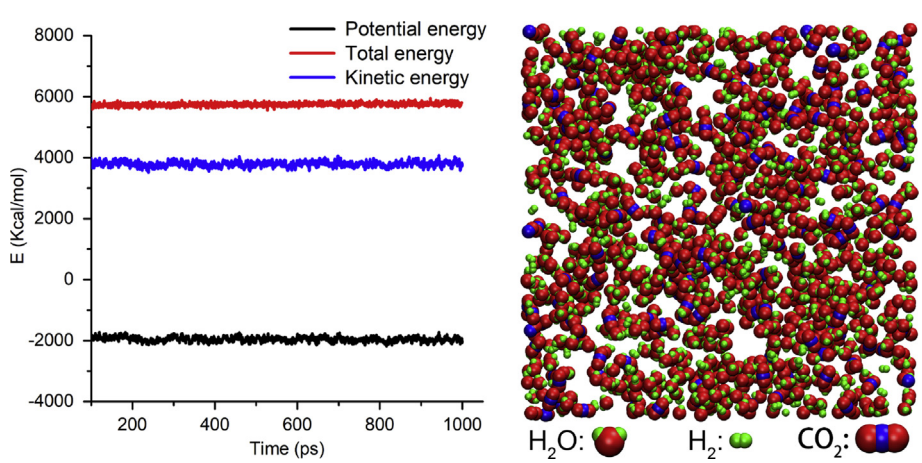

Fig. 6 – Energy (a) and final snapshots (b) for $H_2O/H_2/CO_2$ ternary mixtures at 673 K. ($x_{H_2} = x_{CO_2} = 14.2\%$, v = 0.182 L/mol). Carbon atoms, oxygen atoms and hydrogen atoms are in blue, red and green color in the snapshots, respectively. (For interpretation of the references to color/colour in this figure legend, the reader is referred to the Web version of this article.)

Table 3 – The simulation results for $H_2O/H_2/CO_2$ mixtures with different system sizes.

Index	v/L mol^{-1}	T/K	[a]$H_2O/H_2/CO_2$	V/ × 10^5 Å^3	P/MPa
1	0.182	673	500/100/100	2.109	24.45±0.059
2			1000/200/200	4.219	24.56±0.041
3			1500/300/300	6.328	24.62±0.032
4			2000/400/400	8.438	24.64±0.028
5			5000/1000/1000	21.140	24.53±0.019
6			10000/2000/2000	42.279	24.55±0.013
1	0.182	773	500/100/100	2.109	31.10±0.055
2			1000/200/200	4.219	31.34±0.039
3			1500/300/300	6.328	31.39±0.031
4			2000/400/400	8.438	31.33±0.027
5			5000/1000/1000	21.140	31.39±0.017
6			10000/2000/2000	42.279	31.37±0.013
1	0.182	873	500/100/100	2.109	37.59±0.059
2			1000/200/200	4.219	37.78±0.040
3			1500/300/300	6.328	37.82±0.033
4			2000/400/400	8.438	37.98±0.028
5			5000/1000/1000	21.140	37.73±0.019
6			10000/2000/2000	42.279	37.75±0.013
1	0.182	973	500/100/100	2.109	43.89±0.058
2			1000/200/200	4.219	43.75±0.042
3			1500/300/300	6.328	43.74±0.033
4			2000/400/400	8.438	43.97±0.029
5			5000/1000/1000	21.140	43.78±0.019
6			10000/2000/2000	42.279	43.80±0.013

[a] Numbers of H_2O, H_2, and CO_2 molecules.

marginal, which is agreement with the conclusion by Zhang et al. [33]. The system size we adopted in our simulations (1000 H_2O molecules) can give a good balance of accuracy and efficiency for the simulations.

Fig. 7(a)–(d) show the predicted PVT properties for $H_2O/H_2/CO_2$ ternary mixtures by the MD simulations and the PR equation of state at different temperatures and molar volumes. The temperatures range from 673 to 973 K, and the molar volumes are 0.182 L/mol, 0.435 L/mol, 0.833 L/mol, and 1.429 L/mol, respectively. The pressure is predicted for the ternary mixtures with molar fractions of H_2 and CO_2,x_{H_2},x_{CO^2} = 4.5%, 8.3%, 11.5%, and 14.2% at each fixed temperature and molar volume, respectively.

The ARDs between the MD simulation results and calculation results by the PR equation of state are compared in Fig. 8(a)–(d). Both the data and corresponding ARD in Figs. 7 and 8 are provided in Table S4 of the Supporting information. The ARDs between the MD simulation results and the calculation results by the PR equation of state at 673 K are relatively large, especially whenx_{H_2},x_{CO^2} = 4.5%. When molar volumes increase from 0.182 L/mol to 1.429 L/mol, the maximum ARDs decrease with the following values: 18.7%, 8.4%, 6.6%, and 5.2%. The large ARDs should mainly come from the limited accuracy of the standard PR equation of state [57,58]. Further analysis of the ARDs has not been possible primarily because of the lack of experimental data.

The compression factors have been successfully used to describe the deviation from ideal gas behavior for a real gas or mixture. Using the simulation results of the PVT properties for $H_2O/H_2/CO_2$ ternary mixtures and Eq. (17), the corresponding compression factors are calculated and shown in Fig. 9. It can be observed that the mixture behaves more nearly like an ideal gas with the increasing of the temperature. Moreover, the effect of the molar fraction of H_2 and CO_2 on the compression factor is getting smaller and smaller as the temperature increases.

Since the MD method is insensitive to the state of the mixture, the prediction results shown in Fig. 8 should be more believable than those determined from the standard PR equation of state near the critical point of the water. In fact, in Fig. 7(a)–(d) (or Fig. 8 (a)–(d)), as the temperature increases from 673 K to 973 K at each molar volume, the state of the $H_2O/H_2/CO_2$ ternary mixtures after equilibrium gradually approaches more and more closely to the ideal gas state. To make it more clear, we calculate the radial distribution function (RDF) of the $H_2O/H_2/CO_2$ ternary mixtures for the MD simulations at each temperature from 673 K to 973 K with $x_{H_2} = x_{CO^2}$s = 14.2%, v = 0.182 L/mol, as shown in Fig. 10.

The RDF (also called g(r)) describes how density varies as a function of distance from a reference particle. Fig. 10(a) shows the total RDF which is computed including the contributions from all atom pairs in the system. In fact, the $g(r)_{total}$ can be considered as the weighted sum of g(r) for all the different atom pairs. As observed in Fig. 10(a), the RDFs have a single peak at the nearest-neighbor distance 3.41 Å, and the $g(r)_{total}$ shows a fast decay to 1 after the peak. Moreover, with the increase of the temperature, the amplitude of the peaks decreases with the increase of the temperature, and the system gradually approaches the ideal gas state.

In fact, the typical state of the $H_2O/H_2/CO_2$ ternary mixtures at temperatures ranging from 673 K to 973 K can be described more clearly in Fig. 10(b), (c), and (d), which depict $g(r)_{O(H_2O)-O(H_2O)}$, $g(r)_{O(H_2O)-H(H_2O)}$and $g(r)_{O(H_2O)-H(H_2)}$, respectively. The RDFs show that the H_2O, CO_2, and H_2 molecules are

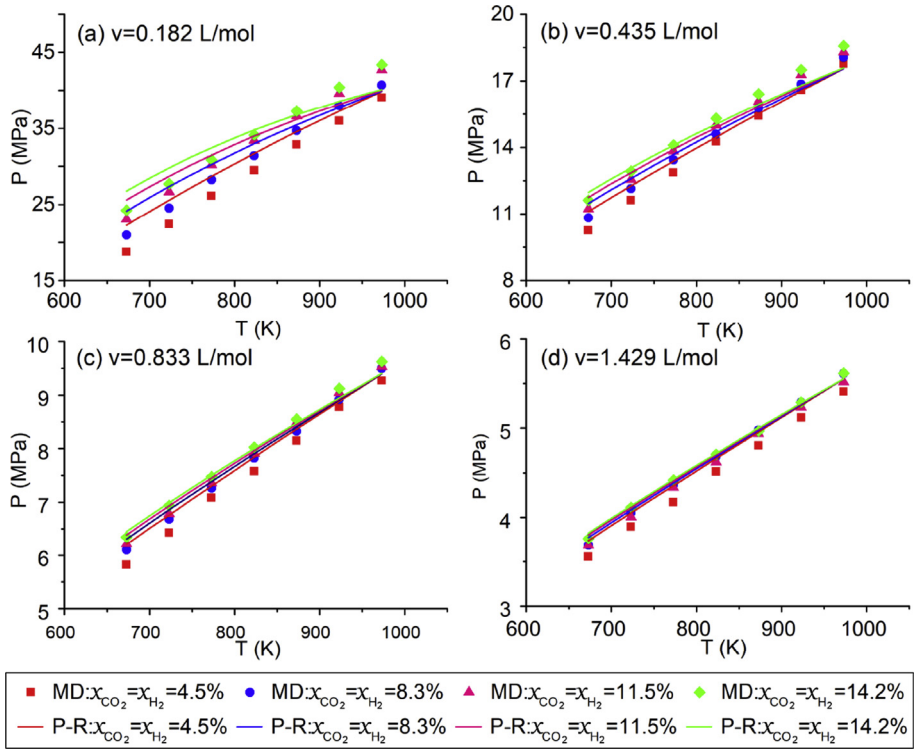

Fig. 7 – Pressure as a function of temperature predicted by the molecular dynamics simulation compared with the theoretical calculation for $H_2O/H_2/CO_2$ ternary mixtures at different molar volumes.

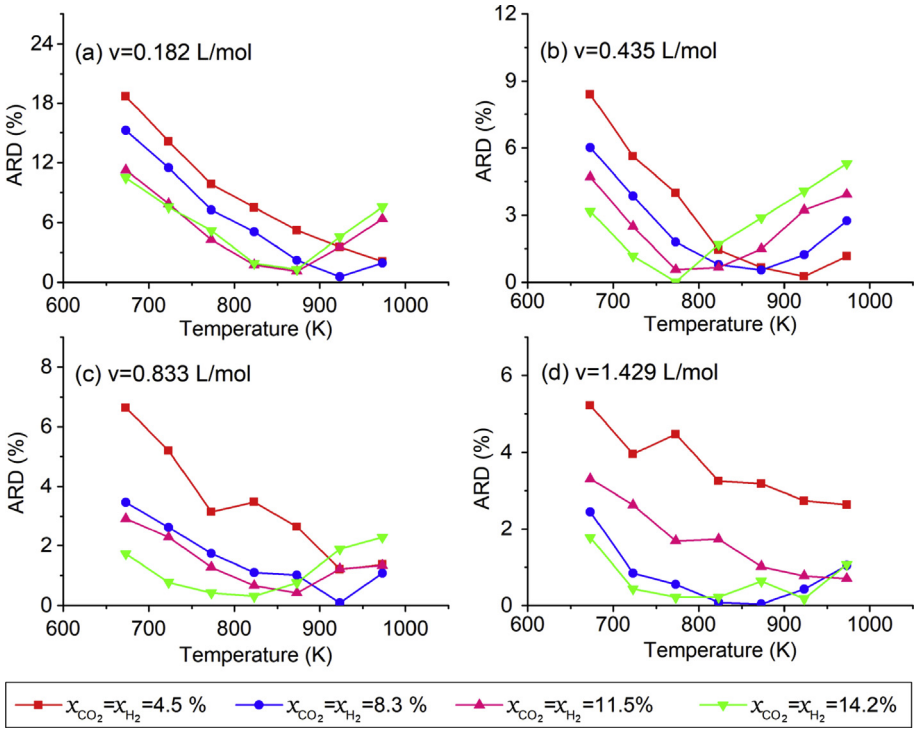

Fig. 8 – ARD as a function of temperature predicted by the molecular dynamics simulation compared with the theoretical calculation for $H_2O/H_2/CO_2$ ternary mixtures at different molar volumes.

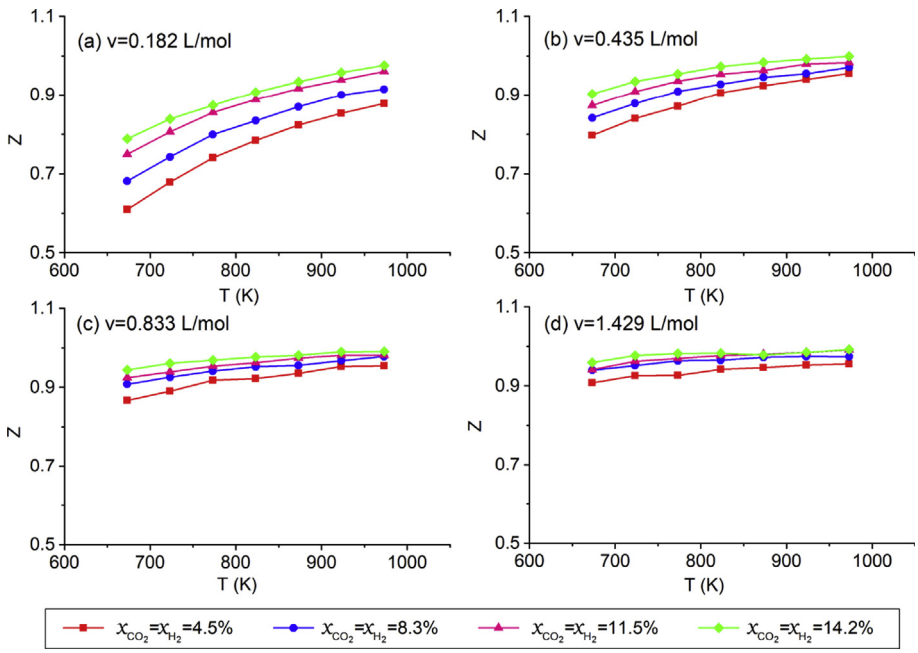

Fig. 9 – Compression factor as a function of temperature for $H_2O/H_2/CO_2$ mixtures at different molar volume.

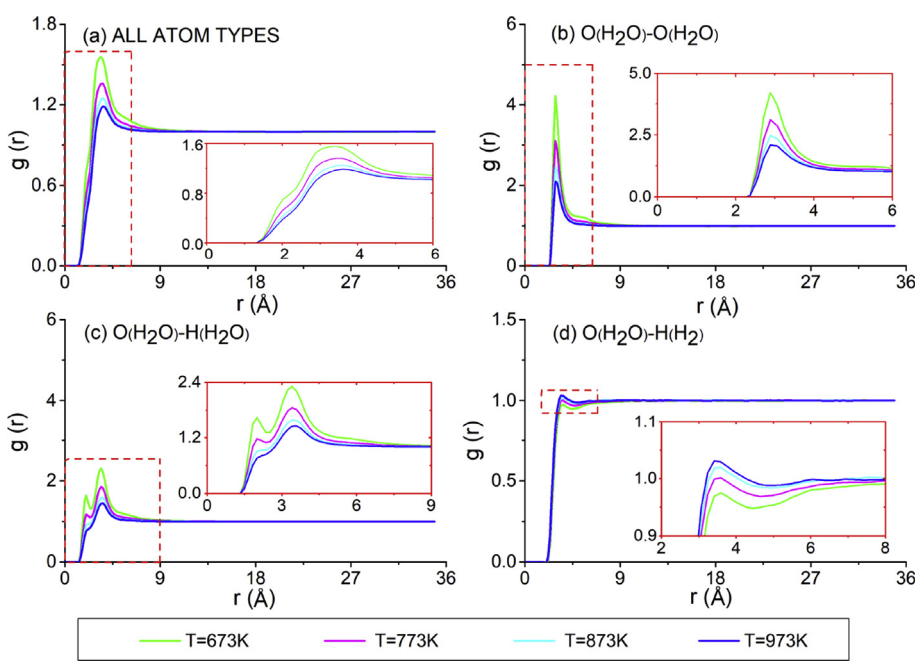

Fig. 10 – RDF between different atom types for $H_2O/H_2/CO_2$ mixtures: (a) RDF for all atom types; (b) RDF for $O(H_2O)$-$O(H_2O)$; (c) RDF for $O(H_2O)$-$H(H_2O)$; (d) RDF for $O(H_2O)$-$H(H_2)$. ($x_{H_2} = x_{CO^2} = 14.2\%$, $v = 0.182$ L/mol).

randomly distributed in thermodynamic states. The peaks of $g(r)_{O(H_2O)-O(H_2O)}$ at approximately 2.89 Å indicate that they are in the"hydrogen-bonding" regions [59], and also indicate the presence of amounts of small hydrogen-bonded cluster [59,60]. $g(r)_{O(H_2O)-H(H_2O)}$ shows O-H distances for neighboring H_2O molecules, and the first peaks locates at about 2.0 Å, which are shorter than the sum of Van der Waals radii of the oxygen and hydrogen atoms of 2.7 Å. With the increase of the temperature, the amplitude of the peaks for $g(r)_{O(H_2O)-O(H_2O)}$, $g(r)_{O(H_2O)-H(H_2O)}$decrease gradually, and the first peaks of $g(r)_{O(H_2O)-H(H_2O)}$even becomes a insignificant shoulder at its place. These indicate that the size of small clusters and the average number of H-bonds per molecule decrease with increasing temperature, which agree well with the findings for Hydrogen-Bonded clusters in pure water previously reported by Kalinichev [59] and Swiatla-Wojcik et al. [60].

Conclusions

In summary, the PVT properties of $H_2O/H_2/CO_2$ mixtures in the near-critical and supercritical regions of water are investigated using molecular dynamics simulations and the PR equation of state. First, the molecular dynamics simulations of PVT properties for H_2O/CO_2 binary mixtures and the theoretical calculations based on the PR equation of state are carried out, and the obtained results are compared with the experimental values. The analysis shows that the results of the molecular dynamics simulations match the experimental values better than those calculated by the PR equation of state in near-critical and supercritical regions of water. Then, the PVT properties of H_2O/H_2 binary mixtures and $H_2O/H_2/CO_2$ ternary mixtures are predicted by MD simulations and calculated by the PR equation of state. The adopted MD simulations could provide more insight into the mechanism than the PR equation of state in predicting PVT properties of H_2O/H_2 binary mixtures and $H_2O/H_2/CO_2$ ternary mixtures in the near-critical and supercritical regions of water.

The PVT properties for $H_2O/H_2/CO_2$ mixtures are essential to the design and optimization of a thermodynamic system based on coal and supercritical water gasification; to date, however, no experimental, theoretical, or simulation research has been conducted on the PVT properties for $H_2O/H_2/CO_2$ in the near-critical and supercritical regions of water. In the current work, the PVT properties for $H_2O/H_2/CO_2$ mixtures are obtained by MD simulations and the PR equation of state; thus, the findings could offer useful guidelines for experimental measurement in the future. Moreover, the results of this paper are of great significance to the development of supercritical water gasification of coal, and could offer remarkable value for the application of $H_2O/H_2/CO_2$ mixtures in practical production.

Acknowledgments

This work was supported by the National Key R&D Program of China (Grant No. 2016YFB0600100).

Appendix A. Supplementary data

Supplementary data related to this article can be found at https://doi.org/10.1016/j.ijhydene.2018.04.214.

REFERENCES

[1] Huang B, Xu S, Gao S, Liu L, Tao J, Niu H, et al. Industrial test and techno-economic analysis of CO_2 capture in Huaneng Beijing coal-fired power station. Appl Energy 2010;87:3347–54.
[2] Majoumerd MM, De S, Assadi M, Breuhaus P. An EU initiative for future generation of IGCC power plants using hydrogen-rich syngas: simulation results for the baseline configuration. Appl Energy 2012;99:280–90.
[3] Xu CG, Cai J, Li XS, Lv QN, Chen ZY, Deng HW. Integrated process study on hydrate-based carbon dioxide separation from integrated gasification combined cycle (IGCC) synthesis gas in scaled-up equipment. Energy Fuel 2012;26:6442–8.
[4] Chandra D, Elsworth D, VanEssendelft D. Mechanical and transport characteristics of coal-biomass mixtures for advanced IGCC systems. Energy Fuel 2012;26:5729–39.
[5] Botero C, Field RP, Brasington RD, Herzog HJ, Ghoniem AF. Performance of an IGCC plant with carbon capture and coal-CO_2-slurry feed: impact of coal rank, slurry loading, and syngas cooling technology. Ind Eng Chem Res 2012;51:11778–90.
[6] Chen W, Xu R. Clean coal technology development in China. Energy Pol 2010;38:2123–30.
[7] Lanzi E, Verdolini E, Haščič I. Efficiency-improving fossil fuel technologies for electricity generation: data selection and trends. Energy Pol 2011;39:7000–14.
[8] Guo L, Jin H. Boiling coal in water: hydrogen production and power generation system with zero net CO_2 emission based on coal and supercritical water gasification. Int J Hydrogen Energy 2013;38:12953–67.
[9] Li Y, Guo L, Zhang X, Jin H, Lu Y. Hydrogen production from coal gasification in supercritical water with a continuous flowing system. Int J Hydrogen Energy 2010;35:3036–45.
[10] Jin H, Lu Y, Liao B, Guo L, Zhang X. Hydrogen production by coal gasification in supercritical water with a fluidized bed reactor. Int J Hydrogen Energy 2010;35:7151–60.
[11] Zhang J, Weng X, Han Y, Li W, Cheng J, Gan Z, et al. The effect of supercritical water on coal pyrolysis and hydrogen production: a combined ReaxFF and DFT study. Fuel 2013;108:682–90.
[12] Zhang J, Weng X, Han Y, Li W, Gan Z, Gu J, et al. Effect of supercritical water on the stability and activity of alkaline carbonate catalysts in coal gasification. J Energy Chem 2013;22:459–67.
[13] Jin H, Chen Y, Ge Z, Liu S, Ren C, Guo L. Hydrogen production by Zhundong coal gasification in supercritical water. Int J Hydrogen Energy 2015;40:16096–103.
[14] Lan R, Jin H, Guo L, Ge Z, Guo S, Zhang X. Hydrogen production by catalytic gasification of coal in supercritical water. Energy Fuel 2014;28:6911–7.
[15] Su X, Jin H, Guo L, Guo S, Ge Z. Experimental study on Zhundong coal gasification in supercritical water with a quartz reactor: reaction kinetics and pathway. Int J Hydrogen Energy 2015;40:7424–32.
[16] Ge Z, Guo L, Jin H. Hydrogen production by non-catalytic partial oxidation of coal in supercritical water: the study on reaction kinetics. Int J Hydrogen Energy 2017;42:9660–6.
[17] Guo L, Jin H, Lu Y. Supercritical water gasification research and development in China. J Supercrit Fluids 2015;96:144–50.
[18] Ohsumi T, Nakashiki N, Shitashima K, Hirama K. Density change of water due to dissolution of carbon dioxide and near-field behavior of CO2, from a source on deep-sea floor. Energy Convers Manag 1992;33:685–90.
[19] Zhang Z, Duan Z. Phase equilibria of the system methane–ethane from temperature scaling gibbs ensemble Monte Carlo simulation. Geochim Cosmochim Acta 2002;66:3431–9.
[20] Hebach A, Oberhof A, Dahmen N. Density of water + carbon dioxide at elevated pressures: measurements and correlation. J Chem Eng Data 2004;49:950–3.
[21] Singh J, Blencoe JG, Anovitz LM. Volumetric properties and phase relations of binary H_2O-CO_2-CH_4-N_2 mixtures at 300 °C and pressures to 1000 bars. In: Steam, water, and hydrothermal systems: physics and chemistry meeting the needs of industry. Ottawa, Canada: NRC Research Press; 2000. p. 134–43.

[22] Seitz JC, Blencoe JG. Experimental determination of the volumetric properties and solvus relations of H_2O-CO_2 mixtures at 300–400°C and 75–1000 bars. In: The fifth international symposium on hydrothermal reactions; 1997. p. 109–12.

[23] Asahara Y, Murakami M, Ohishi Y, Hirao N, Hirose K. Sound velocity measurement in liquid water up to 25GPa and 900K: implications for densities of water at lower mantle conditions. Earth Planet Sci Lett 2010;289:479–85.

[24] Guo T, Hu J, Mao S, Zhang Z. Evaluation of the pressure–volume–temperature (PVT) data of water from experiments and molecular simulations since 1990. Phys Earth Planet Int 2015;245:88–102.

[25] Dohrn R, Brunner G. High-pressure fluid-phase equilibria: experimental methods and systems investigated. Fluid Phase Equil 1988–1993;1995(106):213–82.

[26] Kato K, Nagahama K, Hirata M. Generalized interaction parameters for the Peng-Robinson equation of state: carbon dioxide-n-paraffin binary systems. Fluid Phase Equil 1981;7:219–31.

[27] Adrian T, Wendland M, Hasse H, Maurer G. High-pressure multiphase behaviour of ternary systems carbon dioxide–water–polar solvent: review and modeling with the Peng-Robinson equation of state. J Supercrit Fluids 1998;12:185–221.

[28] Belonoshko A, Saxena SK. A molecular dynamics study of the pressure-volume-temperature properties of super-critical fluids: I. H_2O. Geochim Cosmochim Acta 1991;55:381–7.

[29] Belonoshko A, Saxena SK. A molecular dynamics study of the pressure-volume-temperature properties of supercritical fluids: II. CO_2, CH_4, CO, O_2, and H_2. Geochim Cosmochim Acta 1991;55:3191–208.

[30] Duan Z, Møller N, Weare JH. A general equation of state for supercritical fluid mixtures and molecular dynamics simulation of mixture PVTX properties. Geochim Cosmochim Acta 1996;60:1209–16.

[31] Duan Z, Zhang Z. Equation of state of the H_2O, CO_2, and H_2O–CO_2 systems up to 10 GPa and 2573.15 K: molecular dynamics simulations with ab initio potential surface. Geochim Cosmochim Acta 2006;70:2311–24.

[32] Berendsen HJC, Grigera JR, Straatsma TP. The missing term in effective pair potentials. J Phys Chem 1987;91:6269–71.

[33] Zhang Z, Duan Z. Prediction of the PVT properties of water over wide range of temperatures and pressures from molecular dynamics simulation. Phys Earth Planet In 2005;149:335–54.

[34] Vorholz J, Harismiadis VI, Rumpf B, Panagiotopoulos AZ, Maurer G. Vapor+liquid equilibrium of water, carbon dioxide, and the binary system, water+carbon dioxide, from molecular simulation. Fluid Phase Equil 2000;170:203–34.

[35] Shvab I, Sadus RJ. Thermophysical properties of supercritical water and bond flexibility. Phys Rev E 2015;92:012124.

[36] Potoff JJ, Siepmann JI. Vapor–liquid equilibria of mixtures containing alkanes, carbon dioxide, and nitrogen. Aiche J 2001;47:1676–82.

[37] Harris JG, Yung KH. Carbon dioxide's liquid-vapor coexistence curve and critical properties as predicted by a simple molecular model. J Phys Chem 1995;99:12021–4.

[38] Brodholt J, Wood B. Molecular-dynamics simulations of the properties of CO_2-H_2O mixtures at high-pressures and temperatures. Am Mineral 1993;78:558–64.

[39] Cracknell RF. Molecular simulation of hydrogen adsorption in graphitic nanofibres. Phys Chem Chem Phys 2001;3:2091–7.

[40] Buch V. Path integral simulations of mixed para-D2 and ortho-D2 clusters: the orientational effects. J Chem Phys 1994;100:7610–29.

[41] Allen MP, Tildesley DJ. Computer simulation of liquids. Oxford University Press; 2017.

[42] Kong CL. Combining rules for intermolecular potential parameters. II. Rules for the Lennard-Jones (12–6) potential and the Morse potential. J Chem Phys 1973;59:2464–7.

[43] Tafazzoli M, Khanlarkhani A. Study of self-association of water in supercritical CO_2 by Monte Carlo simulation: does water have a specific interaction with CO_2? Fluid Phase Equil 2008;267(2):181–7.

[44] Liu Y, Lafitte T, Panagiotopoulos AZ, Debenedetti PG. Simulations of vapor–liquid phase equilibrium and interfacial tension in the CO2–H2O–NaCl system. AIChE Jl 2013;59(9):3514–22.

[45] Plimpton S. Fast parallel algorithms for short-range molecular dynamics. J Comput Phys 1995;117:1–19.

[46] Peng DY, Robinson DB. A new two-constant equation of state. Ind Eng Chem Fund 1976;15:59–64.

[47] DIPPR-801. Evaluated process design data, public release documentation. American Institute of Chemical Engineers; 2006.

[48] Meng L, Duan YY, Wang XD. Binary interaction parameter k_{ij} for calculating the second cross-virial coefficients of mixtures. Fluid Phase Equil 2007;260:354–8.

[49] Nishiumi H, Gotoh H. Generalization of binary interaction parameters of Peng-Robinson equation of state for systems containing hydrogen. Fluid Phase Equil 1990;56:81–8.

[50] Brodholt JP, Wood BJ. Measurements of the PVT, properties of water to 25 kbars and 1600°C from synthetic fluid inclusions in corundum. Geochim Cosmochim Acta 1994;58:2143–8.

[51] Frost DJ, Wood BJ. Experimental measurements of the properties of H_2O, CO_2, mixtures at high pressures and temperatures. Geochim Cosmochim Acta 1997;61:3301–9.

[52] Wagner W, Cooper JR, Dittmann A, Kijima J, Kretzschmar HJ, Kruse A, et al. The IAPWS industrial formulation 1997 for the thermodynamic properties of water and steam. Trans ASME 2000;122:150–84.

[53] Kretzschmar HJ, Cooper JR, Dittmann A, Friend DG, Gallagher JS, Knobloch K, et al. Supplementary backward equations for pressure as a function of enthalpy and entropy p(h,s) to the industrial formulation IAPWS-IF97 for water and steam. J Eng Gas Turbines Power 2004;128:702–13.

[54] Kretzschmar HJ, Cooper JR, Dittmann A, Friend DG, Gallagher JS, Harvey AH, et al. Supplementary backward equations T (p, h), v (p, h), and T (p, s), v(p, s) for the critical and supercritical regions (region 3) of the industrial formulation IAPWS-IF97 for water and steam. J Eng Gas Turbines Power 2006;129:294–303.

[55] Fenghour A, Wakeham WA, Watson JTR. Densities of (water+carbon dioxide) in the temperature range 415 K to 700 K and pressures up to 35 MPa. J Chem Thermodyn 1996;28:433–46.

[56] Patel MR, Eubank PT. Experimental densities and derived thermodynamic properties for carbon dioxide-water mixtures. J Chem Eng Data 1988;33:185–93.

[57] Smits PJ, Economou IG, Peters CJ, Swaan Arons JD. Equation of state description of thermodynamic properties of near-critical and supercritical water. J Phys Chem C 1994;98(46):12080–5.

[58] Jiang J, Prausnitz JM. Equation of state for thermodynamic properties of chain fluids near-to and far-from the vapor–liquid critical region. J Chem Phys 1999;111:5964–74.

[59] Kalinichev AG. Molecular simulations of liquid and supercritical water: thermodynamics, structure, and hydrogen bonding. Rev Mineral Geochem 2001;42(1):83–129.

[60] Swiatla-Wojcik D, Pabis A, Szala J. Density and temperature effect on hydrogen-bonded clusters in water-MD simulation study. Cent Eur J Chem 2008;6(4):555–61.